iPSC based clinical translation of phenotype and pharmacology in primary erythromelalgia, an inherited chronic pain condition.

Lishuang Cao[1]*, Aoibhinn McDonnell[1]*, Anja Nitzsche[1]*, Aristos Alexandrou[1], Pierre-Philippe Saintot[1], Alexandre J.C. Loucif[1], Adam R. Brown[1], Gareth Young[1], Malgorzata Mis[2], Andrew Randall[3], Stephen G. Waxman[4], Philip Stanley[1], Simon Kirby[1], Sanela Tarabar[5], Alex Gutteridge[1], Richard Butt[1], Ruth McKernan[1], Paul Whiting[1], Zahid Ali[1†], James Bilsland[1†§], Edward B. Stevens[1†]

Affiliations

[1]. Pfizer Neuroscience and Pain Research Unit, The Portway Building, Granta Park Cambridge CB21 6GS, UK

[2]. University of Bristol, School of Physiology and Pharmacology, Bristol,UK

[3.] Hatherly College of Life and Environmental Sciences, University of Exeter, Prince of Wales Road, Exeter EX4 4PS ,UK

[4.] Centre for Neuroscience & Regeneration Research, Veterans Affairs Medical Center, West Haven, 950 Campbell Avenue ,BLDG. 34,West Haven, CT 0651

[5.]Pfizer 1 Howe St, New Haven, CT 06511, United States§Corresponding author. E-mail: James.Bilsland@pfizer.com

- * Authors contributed equally to the work
- † Authors contributed equally to the work

‡ Present address: Pfizer Neuroscience and Pain Research Unit, The Portway Building, Granta Park, Cambridge CB21 6GS, UK

One sentence summary: Bench to bedside translation using iPSC to characterise phenotype and pharmacology in primary erythromelalgia, an inherited chronic pain condition.

ABSTRACT

In common with other chronic pain conditions, inherited erythromelalgia (IEM) represents a significant unmet medical need. The peripherally expressed *SCN9A* encoded sodium channel Nav1.7 plays a critical role in IEM with gain-of-function leading to aberrant sensory neuronal activity and extreme pain, particularly in response to heat. In five carefully phenotyped IEM patients, a novel highly potent and selective Nav1.7 blocker reduced heat-induced pain in the majority of subjects. In four of the five subjects we used induced pluripotent stem cell (iPSC) technology to create sensory neurons which uniquely emulated the clinical phenotype of hyperexcitability and aberrant responses to heat stimuli. When we compared the severity of the clinical phenotype with the iPSC-derived sensory neuron hyperexcitability we saw a trend towards a correlation for individual mutations. The in vitro IEM phenotype was sensitive to Nav1.7 blockers, including the clinical test agent. Given the importance of peripherally expressed sodium channels in many pain conditions, this translational approach is likely to have broader utility to a wide range of pain and sensory conditions. This emphasizes the use of iPSC approaches to bridge between clinical and preclinical studies, enabling greater understanding of a disease and the response to a therapeutic agent in defined patient populations.

INTRODUCTION

Individual *SCN9A* mutations leading to a loss of channel function have been associated with congenital insensitivity to pain, while gain-of-function mutations in the *SCN9A* gene have been associated with chronic painful conditions including inherited erythromelalgia (IEM),

paroxysmal extreme pain disorder (PEPD) and idiopathic small fibre neuropathy (iSFN). IEM is a chronic extreme pain condition which results in burning pain sensations and erythema, particularly in the distal extremities[1,2,3,4]. The pain is often episodic and mild heat or body temperature rise is a common/major trigger for pain attack in IEM[4].

The development of selective Nav1.7 blockers, in common with other novel analgesic drug targets, has been hampered by the lack of robust preclinical to clinical translation. In particular, a complete understanding of the role of Nav1.7 in action potential firing in human sensory neurons has been limited by the reliance of electrophysiological studies on heterologous expression of the channel. For example, all eighteen reported IEM Nav1.7 mutations are associated with a hyperpolarized activation voltage (with or without concomitant shifts in voltage-dependence of fast inactivation) following heterologous expression in mammalian cell lines[5,6,7,8,9], however, the absolute value and magnitude of changes in gating parameters for individual IEM mutations varies between different laboratories and may not directly translate to native Nav1.7 in human sensory neurons[5,6,10].

Overexpression of Nav1.7 IEM mutations in mouse DRG neurons has been used to understand the contribution of the changes in channel gating to action potential firing properties[11.] The interpretation is, however, compromised by the level of expression of human Nav1.7 relative to rodent TTX-S channels and appropriate processing and assembly of the human isoform in a rodent neuronal background. Human pluripotent stem cell derived sensory neurons[12,13] provide an improved physiologically relevant model to investigate the relationship between a human ion channel in its native environment and neuronal excitability.

Induced pluripotent stem cell technology allows generation of cells from patients, which retain the genetic identity of the donor and can recapitulate disease pathology in differentiated progeny. This has potential to enable novel therapeutics to be tested both on individual patients and their cognate iPSC-derived cells to further understand both clinical efficacy and

effects on the underlying cellular phenotype. However, to date it is unclear to what extent the response of a therapeutic agent in an iPS disease model translates to the clinic, as no such fully translated study has been reported.

In this study, we investigated the effect of a novel selective Nav1.7 blocker PF-05089771 on the inhibition of heat-evoked pain in five IEM subjects carrying four different *SCN9A* mutations. Simultaneously, we generated iPSC based sensory neurons from four of the five IEM subjects, in order to characterize neuronal phenotype associated with individual mutations and the effects of selectively blocking Nav1.7 channels on action potential generation. This study represents the first disease-based phenotypic and pharmacological translation between patient and iPSC neurons derived from those patients, and highlights the unique potential for this approach.

RESULTS

Subject Clinical Information

Five IEM subjects, three males and two females, average age 40.2 years (Table 1) provided informed consent to participate in a double blind, placebo-controlled clinical study. Extensive clinical phenotyping had previously been performed in these subjects[4]. Four of the five subjects additionally consented to donate blood for iPSC generation (Table 1).

IPSC differentiate to functional nociceptive neurons with comparable Nav1.7 expression across all IEM subjects and non-IEM donors

Peripheral blood mononuclear cells were extracted from donated blood samples. The erythroid progenitor populations of the peripheral blood cells were reprogrammed to iPSC and up to three clonal iPSC lines per subject were established. Individual heterozygous mutations in the iPSC were confirmed through Sanger sequencing (Fig. 1A). We also generated iPSC from four independent non-IEM donors which were used as a control group,

where no mutations in Nav1.7 associated with PEPD, IEM or CIP were identified. All iPSC clonal lines showed typical morphology for pluripotent cell colonies and expressed the pluripotency marker Oct4 (Fig. 1B). Array CGH analysis revealed a normal karyotype and comparable number or size of copy number variants between non-IEM donor and IEM subject iPSC for the majority of iPSC clones (Supplementary Fig. 1A, B).

We differentiated iPSC into sensory neurons using a small molecule based protocol as described previously[12,13]. One week after addition of neural growth factors the differentiated cells exhibited a neuronal morphology and stained positive for sensory neuron markers Brn3a, Islet1 and Peripherin, with no obvious morphological difference between donor and study subject derived neurons (Fig. 1C). Neurons were further matured for another 8 weeks before electrophysiological recordings were obtained. The sensory neurons derived from non-IEM and IEM clonal iPSC lines all expressed *SCN9A* and other sodium channel subtypes as determined by qPCR (Supplementary Fig. 1C).In order to characterize the functional role of Nav1.7 channel in iPSC-derived sensory neurons (iPSC-SN) using whole-cell patch clamp technique, two selective Nav1.7 blockers were exploited; the clinical compound, PF-05089771 and an in vitro tool, PF-05153462 (Supplementary Fig. 2A, B, C). In comparison to slow kinetics of inhibition for PF-05089771, PF-05153462 displayed fast rates of block and was fully reversible within 10 min, enabling multiple concentrations to be applied to each cell and therefore allowing a more extensive and robust investigation of the contribution of Nav1.7 to sensory neuron excitability.

Application of PF-05153462 reversibly inhibited the peak sodium current of iPSC-SN confirming the functional expression of Nav1.7. Comparison of the Nav1.7 current densities (as defined using inhibition by 100 nM PF-05153462) across iPSC-derived sensory neuron clones revealed no significant differences between the individual clones or between IEM and non-IEM groups (example traces Fig1D; quantification Fig. 1E), non-parametric ANOVA,

P>0.05). In addition, there was no significant difference in the percentage of total sodium current (Supplementary Fig. 3A, non-parametric ANOVA, *P* >0.05) or current carried by Nav1.7 (Supplementary Fig. 3B, non-parametric ANOVA, *P* >0.05) across iPSC-derived sensory neuron clones. These data suggest robust and equivalent expression of Nav1.7 channels in iPSC-SN, irrespective of the donor from which they were generated.

iPSC-SN derived from IEM subjects show elevated level of excitability

We observed spontaneous action potential firing from a sub-population of iPSC-SN at resting membrane potential (Fig. 2A, right). On average the iPSC-SN from IEM donors showed a significantly higher proportion of spontaneously firing cells compared to those from non-IEM donors (*P* <0.05 linear logistic model), suggesting higher excitability (Fig. 2B).

Notwithstanding this, iPSC-SN from subject EM1 (S241T) and non-IEM donor D1 showed similar degrees of spontaneous firing which was only moderately enhanced compared to the other non-IEM donors, suggesting some intrinsic heterogeneity among the iPSC-SN from both the IEM and non-IEM donors (Fig. 2B). There was a small but statistically significant depolarization of resting membrane potential in the IEM subject cells (-57.4 ± 0.4 mV; *N*=272 with all IEM subjects pooled together) compared to non-IEM donor cells (-60 ± 0.4mV; *N*=158 for all non-IEM subjects) (Supplementary Fig. 3C, *P* <0.05 ANOVA), which could contribute to the observed increase in spontaneous activity.

Next, we studied rheobase, the minimal current injection required to evoke an action potential, as a measure of subthreshold contribution to excitability (Fig. 2C). On average, the rheobase was lower in the iPSC-SN from IEM donors (122±10 pA; *N*=270) when compared to neurons from non-IEM donors (361 ± 20 pA; *N*=148) (Fig. 2D, *P* <0.05 non-parametric ANOVA). These data suggest that iPSC-SN from IEM subjects have increased excitability.

We also measured evoked firing frequency in response to increasing amplitude of injected current (Fig. 2E). Although IEM iPSC-SN gave rise to higher number of action potentials at low levels of current injection compared to non-IEM cells (Fig. 2F), there was considerable variability in the firing frequency between cells for each iPSC clone, so this was not considered a reliable endpoint for statistical analysis. Therefore we focused on spontaneous firing and rheobase to determine pharmacological effects of Nav1.7 blockers.

Nav1.7 blockers reduced elevated excitability of IEM iPSC-SN

We further tested the effects of the selective Nav1.7 blocker PF-05153462 on spontaneously firing iPSC-SN (Fig. 3A). As shown in Fig. 3B, the spontaneous firing of iPSC-SN from subjects EM2 (I848T) and EM3 (V400M) was reduced by PF-05153462 in a concentration-dependent manner. IPSC-SN from EM1 (S241T) rarely exhibited spontaneous firing (Fig. 2B); therefore PF-05153462 was not tested. The spontaneous firing in iPSC-SN from EM5 (F1449V) was not sustained for sufficient duration to generate a concentration-response curve, therefore, a single concentration of PF-05153462 (100 nM) was tested and was found to completely inhibit spontaneous firing (data not shown). PF-0508977, the Nav1.7 blocker evaluated in IEM subjects, was also tested on iPSC-SN from EM2, where spontaneous firing was completely blocked at a concentration of 60 nM (Fig. 3C). These data indicate that the gain-of-function mutations present in IEM Nav1.7 channels contribute to the higher incidence of spontaneous firing in iPSC-SN from IEM subjects.

Next we investigated the contribution of wild type (WT) and IEM mutant Nav1.7 channels to rheobase of the action potential using PF-05089771 (Fig. 3D). Voltage-clamp recordings of Nav1.7 EM mutations stably expressed in HEK293 cells resulted in very similar IC_{50}s ranging from 11 nM to 36 nM (Supplementary Fig. 2D). While PF-05089771 increased the rheobase in a concentration-dependent manner for iPSC-SN from both IEM subjects and non-IEM donors (suggesting a clear role of Nav1.7 in setting threshold), the magnitude of this

effect was significantly greater in iPSC-SN derived from IEM subjects at all three concentrations (Fig. 3E, ANOVA P <0.05; N=6 to 10 for each concentration). Similar results were obtained with the selective Nav1.7 blocker PF-05153462 at concentrations greater than 10 nM (Fig. 3F, ANOVA P <0.05; N= 6 to 10 for each concentration). The greater contribution of Nav1.7 to rheobase in sensory neurons from IEM subjects compared to non-EM donors most likely reflects enhanced channel activity as a result of gating shifts associated with S241T, I848T, V400M and F1449V mutations. Taken together, these studies using Nav1.7 blockers strongly suggest that these Nav1.7 gain-of-function IEM mutations underpin the increased excitability of iPSC-SN from IEM subjects.

Selective Nav1.7 blocker reverses the elevated sensitivity to heat in IEM iPSC-SN

Action potential rheobase was tracked when the temperature was raised from 35 °C to 40 °C (Fig. 4A, B). In contrast to iPSC-SN from non-IEM donors , the iPSC-SN from IEM subjects exhibited a significant decrease in rheobase in response to the modest temperature increase at group level (P <0.01, ANOVA; N=13 to 34), indicating higher excitability of the IEM neurons upon heat stimulation. Interestingly, EM1 appears to be an outlier with similar temperature sensitivity to healthy donor clones. These data suggest that the gain-of-function Nav1.7 mutations in the iPSC-SN from IEM subjects confer an increase in excitability in response to heating at innocuous temperatures. As shown in Fig. 4C-D, 100 nM PF-0515462 was able to reverse the effect of increasing temperature on the rheobase in iPSC-SN from subjects EM2 (I848T), EM3 (V400M) and EM5 (F1449V) (P <0.05 paired t test; N=6 to 11) in cells with a positive rheobase response (>50 pA) to PF-05153462 at 35 °C (an indication of the functional expression of Nav1.7). These data suggest that Nav1.7 underlies the temperature sensitivity in IEM iPSC.

The change in temperature sensitivity following compound application was plotted against the effect of compound on rheobase at 35 °C, and a positive correlation was observed in

iPSC-SN from all EM subjects (Pearson's r=0.22, 0.88, 0.82 and 0.77 respectively). The regression coefficients were significantly different from zero for iPSC-SN from subjects EM2 (I848T), EM3 (V400M) and EM5 (F1449V), suggesting that the amplitude of rheobase changes in response to heat was a function of available Nav1.7 conductance (Fig. 5). This effect was not evident in iPSC-SN from subject EM1. Wild Type (WT) Nav1.7 channels were also temperature-dependent (Supplementary Fig. 4). Taken together, this analysis suggests Nav1.7 is the major contributor for the elevated heat sensitivity in IEM iPSC-SN.

Clinical Efficacy of the Nav1.7 selective blocker PF-05089771

IEM subjects were randomized to participate in two independent treatment sessions (each consisting of two study periods), and to receive a single oral dose of either the Nav1.7 blocker PF-05089771 or matched placebo in a crossover manner during each session (Fig. 6A). Evoked pain attacks were induced in subjects using a controlled heat stimulus applied to the extremities immediately before dosing, as well as at intervals up to 24 hr postdose in each study period (Fig. 6B). Blood samples collected from subjects for pharmacokinetics analysis showed that peak plasma concentrations of PF-05089771 were obtained at 4-6 hr postdose (Supplementary Fig. 5).

Subjects rated their pain using a pain intensity numerical rating scale (PI-NRS) where 0 = no pain and 10= the worst pain possible. A pain attack with a PI-NRS score of at least 5 was evoked prior to dosing with PF-05089771 or placebo. Efficacy endpoints included the average and maximum pain scores in response to evoked heat at 0-4 hr, 4-5 hr, 8-9 hr and 24-25 hr after dosing.

Individual subject maximum pain scores and change from baseline pain scores postdose are shown in Fig. 6C,D. Maximum pain score results postdose (Fig. 6E) were similar, irrespective of whether cooling therapy (used by subjects EM2 [I848T] and EM4 [V400M]) was administered in the interval before evoking a pain attack. The p-values for the

comparison of PF-05089771 versus placebo are 0.04 at 4-5 hr and 0.08 at 8-9 hr when subjects who used cooling as a rescue therapy are excluded. When subjects who used cooling as a rescue therapy are included the corresponding p-values are 0.06 and 0.03. There was no statistically significant treatment effect for PF-05089771 versus placebo at the 0-4 hr timepoint.

PF-05089771 was well tolerated in all subjects, with all treatment-related adverse events classified as mild. The most common treatment-related adverse events were perioral paresthesia, facial flushing and dizziness (Supplementary Table 1).

DISCUSSION

Human iPSC derived disease models are commonly used for the identification or validation of drugs to treat specific disease phenotypes[14,15], yet the degree of translation of drug efficacy to the clinical disease state remains unexplored. Here we show translation of a human pain phenotype and clinical effects of a novel selective Nav1.7 blocker to the preclinical iPSC based disease model from a small cohort of IEM subjects harbouring different mutations in *SCN9A*.

The IEM subject cohort had four different mutations in SCN9A and exhibited pain with multiple characteristics, making it an ideal population for a qualitative, proof-of-concept translational study to assess both phenotype and its reversal through selective Nav1.7 blockade. The Nav1.7 blocker used, PF-05089771, shows greater selectivity for Nav1.7 over all other sodium channel isoforms compared to other sodium channel blockers such as carbamazepine[16] and XEN-402[17,18] .A well-controlled heat stimulus triggered pain attacks in the IEM subject cohort and reproduced many of the features of a natural heat-evoked pain attack[4]. The magnitude of heat-induced pain attacks at 4-5 hr and 8-9 hr was reduced in the majority of the five subjects during at least one of the treatment sessions when dosed with PF-

05089771 compared to subjects who received placebo, confirming efficacy in this proof-of-concept study for the treatment of IEM with a selective Nav1.7 blocker. The shorter duration of the evoked pain attacks (usually less than 1 hr compared to the longer duration recorded in the natural history study[4] and the timing of peak plasma concentration and Tmax of PF-04089771 postdose may account for the lack of treatment response at the 0-4 hr and 24-25 hr timepoints. There appeared to be a degree of variability in response across subjects and between treatment sessions. These observations may be accounted for by the limitation of a single dose study.. . IPSC derived from these subjects provided a unique means to directly evaluate the efficacy of PF-05089771 blockade on the phenotypes of these channel mutations in human sensory neurons.

The increased excitability of iPSC-SN from IEM subjects was not associated with increased expression of Nav1.7, however the mean resting membrane potential of iPSC-SN from IEM subjects was moderately depolarized compared to neurons from the non-IEM donor group. This elevated excitability is likely to be due to an increase in Nav1.7 subthreshold current as modelled by Vasylyev *et al.*,[19]. Overexpression of F1449V, V400M, I848T and S241T Nav1.7 mutants in rodent DRG neurons has also been reported to reduce current threshold and increases the frequency of firing of DRG neurons in response to graded stimuli[20,21,22]. The pathophysiological consequence of IEM on neuronal excitability has been examined in clinical microneurography studies[23,24]. One subject with the I848T mutation demonstrated increased C-fiber nociceptor excitability[25]. The microneurography recordings from human nerve and the excitability measurements in iPSC-derived sensory neurons from patients carrying the same Nav1.7 mutation (I848T) support a role for sensory neuron hyperexcitability underlying the symptoms of IEM.

Direct proof for a role of Nav1.7 in hyperexcitability of sensory neurons from IEM subjects is provided by the use of two Nav1.7 blockers. Both of these compounds have a greater effect

on the rheobase of iPSC-derived sensory neurons from the IEM subject group compared to non IEM donor group, and both compounds reduced spontaneous activity of iPSC-derived sensory neurons from IEM subjects. These data provide the first evidence from native human Nav1.7 channels in human-derived sensory neurons that Nav1.7 mutations associated with IEM lead to a gain-of-function phenotype.

Of particular interest is subject EM1 (S241T). The iPSC-SN from this subject were less excitable than other iPSC-derived neurons from the other IEM subjects in the study, yet the effect of the Nav1.7 blockers on rheobase were equivalent across all IEM iPSC-derived neurons, confirming the Nav1.7 gain-of-function phenotype. Furthermore, although the majority of IEM derived neurons were more excitable in response to heat in accordance with the clinical phenotype, PF-05153462 only blocked the heat evoked response in EM2 (I848T), EM3 (V400M) and EM5 (F1449V)-derived sensory neurons, demonstrating that these Nav1.7 mutations contribute to an enhanced temperature-sensitivity. In contrast, there was no effect of temperature on EM1 (S241T). It is possible that the lack of response of heat-evoked pain in EM1 (S241T) to PF-05089771 in the clinic could be related to the lack of Nav1.7 temperature-dependence at the temperatures tested in iPSC-SN. Age of IEM onset was delayed (17 years old) in subject EM1 (S241T) compared to the other IEM subjects. Previously published studies also report that for S241T, the age of onset was between 8-10 years old (for four out of six affected members[26]) in comparison to early onset (from infancy until 6 years old), with mutations V400M, F1449V and I848T[16,20]. IEM mutations with delayed onset are associated with smaller shifts in gating and reduced hyperexcitability compared to onset in early childhood[21].

The lower excitability of sensory neurons derived from iPSC from subject EM1 carrying S241T may reflect the delayed onset of IEM, either due to differences in Nav1.7 biophysics or different processing of Nav1.7 during cell maturation relative to the other IEM mutants. It

is not appropriate to draw a clear cause –effect relationship between the complex individual subject clinical phenotype and the phenotype of the cognate iPSC-SN; nevertheless, it is interesting to note that subject EM1 (S241T) had the mildest clinical phenotype and their iPSC derived sensory neurons were the least excitable of the IEM derived cell lines, while in contrast subject EM2 (I848T) had a more severe clinical phenotype and their iPSC-SN were highly excitable. With this apparent translation of phenotype and treatment response from clinical study subject to the cognate iPSC disease model, it will be interesting to further decipher underlying mechanism of the variation.

It is also interesting to note the range of excitability within the iPSC-SN from the four non-IEM donors. Further studies are required to determine the degree of variation in excitability of sensory neurons across the normal human population and its biological basis.

Our data demonstrate utility of Nav1.7 blockers for the treatment of pain caused by IEM and the utility of iPSC-SN for recapitulation of sensory nerve fibre dysfunction in vitro. Our results also highlight differences in the effect of the clinical compound in cells derived from non-IEM donors relative to IEM subjects. Thus, iPSC-SN may further assist in the understanding of certain pain conditions and potential pharmacoresponsiveness of individuals to established and novel treatments using a personalised treatment approach. There are, however, some limitations to this work. Inherited erythromelalgia is a rare disease; as a result, the number of eligible subjects in the clinical study was small, representing four different mutations. As the study involved a single dose of compound it was not possible to generate dose response information. The free plasma concentrations of PF-05089771 in the clinical study reached levels which would have been expected to fully inhibit Nav1.7 activity. Given the selectivity profile of the compound, there may also have been limited activity at other peripherally expressed sodium channels, such as Nav1.6. Prior to use in clinical practice, these results may need to be extended to additional IEM subjects particularly those *SCN9A*

gain of function mutations that have not been characterised in the current study. Future studies may also look to extend these results to other *SCN9A*-associated pain conditions such as PEPD and iSFN. In addition, it may be possible to extend these results to more general chronic pain conditions in which *SCN9A* mutations associated with a gain of function of the Nav1.7 channel may contribute to the pain in subgroups of subjects. In summary, this study demonstrates the successful utility of iPSC technology to bridge between clinical and preclinical studies, enabling an understanding of both the disease and the response to a therapeutic agent.

MATERIALS AND METHODS

Clinical Study Design

This was a single center, two-part randomized double-blind third party open placebo controlled exploratory crossover study (Fig. 6A). All subjects provided informed consent in accordance with ethical principles originating in, or derived from the Declaration of Helsinki 2008 prior to undergoing study-related procedures. This study was reviewed and approved by an Independent Ethics Review Board.

Subjects 18 to 78 years of age with a clinical and genetic diagnosis of IEM were eligible to participate in this study. Subjects were excluded if they had other clinically significant illnesses or were unable to wash out of, and to refrain from using concomitant pain medications during the study such as carbamazepine, lamotrigine, oxcarbazepine, mexiletine and amitryptiline, capsaicin patches and local anesthetic patches and oral/injectable corticosteroids. All subjects washed out of their concomitant pain medications prior to taking part in the study. To manage pain due to their IEM during the study, subjects were permitted to use non-pharmacological therapy such as cooling the extremities, or acetaminophen (up to a maximum of 3000 mg/day).

The five subjects enrolled in this study had participated in a previous non-drug clinical phenotyping study in which the triggers for pain attacks and the duration, intensity and frequency of pain attacks and ongoing pain between attacks (if any) were recorded by subjects in a pain diary on a daily basis over a three month period[4]. Pain attacks occurred primarily in the feet and hands and the principal triggers for evoking pain attacks were warmth or heat, exercise and environmental factors (usually hot and/or humid weather)[4].

The primary objective of the drug study was to evaluate the overall pain intensity over 4 hr after a single 1600 mg oral dose of PF-05089771 against placebo in subjects experiencing either experimentally evoked (heat stimulation) pain or spontaneous pain due to IEM. Secondary objectives of the study were to evaluate the overall duration, maximum pain intensity and duration of pain intensity (evoked or spontaneous pain) in subjects at 4-5 hr, 8-9 hr and 24-25 hr postdose. Use of, and time to use of pharmacological therapy such as acetaminophen, or non-pharmacological therapy such as cooling the extremities to relieve IEM pain during the study ("rescue therapy") was also recorded.

Part A, the first part of the study, was conducted over one to two days as an in-clinic stay to establish clinical reproducibility and reliability of evoking pain in each subject prior to entering Part B, an extended in-clinic stay in which a single oral dose of study drug or matched placebo was administered. Subjects were randomized into Part B of the study provided they satisfied all subject selection criteria and had a self-reported spontaneous or evoked pain score of ≥ 5 on the PI-NRS (where 0 = no pain and 10 = worst pain possible), prior to dosing. Treatment Session 1 (TS1) and TS2 could be run consecutively, with a minimum 72 hr washout period between the last study treatment in TS1 and the first study treatment in TS2, and a maximum period of up to 6 months between TS1 and TS2, to facilitate enrolment.

The Medi-therm® III MTA 7900 (Stryker, Kalamazoo, MI) device was used as a heating device to evoke pain, as a cooling device for the cooling paradigm part of the study and as means to deliver non-pharmacological cooling of the extremities as rescue therapy. The Medi-Therm® device supplied cold or warm water at operator-determined temperatures through the use of water circulating thermo-regulated blankets applied to the feet and/or hands or body wraps which were applied to the trunk. The hands and feet, including toes, were completely enclosed in the thermal blankets which were applied in a consistent manner to each subject. Subjects rated their baseline pain score using the PI-NRS. If the subject reported any ongoing pain, attempts were made to reduce the subject's pain score to ≤ 3 on the PI-NRS using a cooling paradigm. Thermal blankets were applied to the subject's extremities (feet and/or hands) and the Meditherm® blankets cooled to 20 °C (cooling paradigm) for at least 5 min (maximum 60 min) until the subject's pain score was ≤ 3 on the NRS. Following cooling, the thermal blankets were heated to 33 °C, the starting temperature for all subjects, and the temperature increased incrementally, in 1 to 2 °C steps, at 10-15 minute intervals, to the device maximum of 42 °C. This temperature was used for a maximum duration of 30 min, until a pain attack with a PI-NRS score of ≥ 5 was induced. This methodology was repeated at least one to two times in Part A of the study to establish individual, standardized time and temperature parameters for evoking pain in each subject for Part B, the drug phase of the study. Subjects recorded pain scores every 15 mins for up to 4 hr after a pain attack was evoked.

Part B of the study had two treatment sessions (TS1 and TS2) with each treatment session consisting of two study periods (Fig. 6B). Subjects received a single dose of either PF-05089771 or placebo in each study period. Treatment sessions could be carried out consecutively, with a minimum washout period of at least 72 hr between study treatments, or separated by up to six months. In Part B, subjects' extremities were cooled (C1 to C4; Fig.

6B) to reduce pain score to ≤ 3 on the NRS, followed by heat stimulation to evoke a pain attack (EP1-EP4). Once the subject reported a pain score of ≥ 5 on PI-NRS, as a result of the Meditherm® device heat stimulus, they were randomized to one of two double blind treatment sequences: PF-05089771/placebo or placebo/PF-04089771, each given as a single oral dose during each of the treatment sessions (TS1, 2). To maintain blinding, PF-05089771 and placebo oral doses were matched in appearance and volume. Postdose pain attacks were evoked, using individual standardized parameters established in Part A with the Meditherm® device, at 4-5 hr, 8-9 hr and 24-25 hr post dose. Subjects were asked to refrain from taking acetaminophen or non-pharmacologic treatments (e.g., Meditherm® cooling function, ice buckets, cold water, cool air fans,) to manage pain until at least 90 min post dose. If acetaminophen or cold therapy were requested by the subject to manage pain, the time, dose (where applicable), duration and frequency of use was recorded. Pain scores were recorded every 5 min for the first hour postdose, then every 15 min until 10 hr postdose. Blood samples were collected for pharmacokinetic and safety laboratory evaluations at pre-specified timepoints postdose. Blood and urine samples for laboratory assessments (hematology, serum chemistry and urinalysis) were collected two days before dosing, 2-4 hr prior to dosing and at 24 hr postdose in each study period. Vital signs were checked two days prior to dosing, 2-4 hr prior to dosing and at 6 hr and 24 hr postdose. ECGs were performed two days before dosing, 2-4 hr prior to dosing and at 8 hr and 24 hr postdose. Adverse events (AEs) were recorded at the time of occurrence from Screening until follow up (28 days after the last dose of study drug).

Collection of Blood for Generation of Induced Pluripotential Stem Cells (iPSC)

Four out of five subjects (Subjects EM1, EM2, EM3 and EM5) consented to an optional procedure to donate blood for generation of iPSC. Approximately 60 ml of blood was collected per subject and aliquoted into six 8 ml Ficoll CPT™ tubes with Sodium Heparin

(Becton Dickinson, Franklin Lakes, New Jersey). The samples were centrifuged at room temperature and mononuclear cells (lymphocytes and neutrophils) harvested to undergo further centrifugation. The centrifuged cells were aspirated and counted using a hemocytometer. Trypan blue was used to identify non-viable cells. Viable cells were resuspended in freezing solution (Human AB serum plus 10% DMSO) to give a final cell density of not more than 50 million cells/ml. Samples were frozen at minus 80 C°.

Clinical Statistical Methods

The primary endpoint, the average heat evoked pain score from 0 - 4hr postdose was analysed using a linear mixed model with terms for baseline, treatment period time postdose, baseline by time postdose interaction, treatment by time postdose interaction and period by time postdose interaction. Subject was included as a random effect in this model. The secondary endpoints of maximum pain score following pain provocation after 4, 8, 10 and 24 hr post dose were analysed using a linear fixed effects model with additive terms for subject, period and treatment. The results are summarised as estimates of treatment effects (PF-05089771 minus placebo) together with 90% confidence intervals.

Maximum pain scores obtained after pain provocation following previous use of rescue therapy were included in the analyses because the rescue medication was non-pharmacological cooling which was also used in the study design to cool subjects if necessary before pain provocation.

EM subject material, generation and maintenance of iPSC

Blood samples from non-IEM donors were obtained from the National Health Service Blood and Transplant (NHSBT) UK. Samples from IEM clinical trial subjects were obtained with their informed consent.

Peripheral Blood Mononuclear Cells (PBMC) were purified using the standard Ficoll-Paque procedure. Cells were expanded into erythroid progenitor cells and transduced with Sendai virus expressing Yamanaka factors OKSM (Life Technologies, Carlsbad, California). IPSC colonies were further expanded to virus-free clonal lines that were cultured and maintained on Matrigel (BD, Oxford, UK) in TeSR1 (STEMCELL Technologies, Vancouver, Canada) and passaged every 6-7 days using Dispase (Life Technologies, Carlsbad, California).

gDNA isolation, Sanger Sequencing and aCGH

Genomic DNA of IEM subject material and iPSC clones was extracted using Qiagen RNA/DNA isolation kit (Qiagen, Hilden, Germany). Segments containing respective mutations were PCR amplified and sequenced for mutation analysis.

Primer sequences (IDT, Coralville, Iowa):

S241T

for: 5'-CATGACTTTCTAGGAAAGCTTGTGT-3'

rev: 5-GTCCAATTAGTGCAAACACACTCA-3'

I848T

for: 5'-ATCATTCAGACTGCTCCGAGTCTT-3'

rev: 5-TTGCAGACACATTCTTTGTAGCTC-3'

S449N

for: 5'-GGGTTTCCTAGGATTTGGAAATGAC-3'

rev: 5'-CTGATGCTGTCCTCTGATTCTGAT-3'

V400M

for: 5'-ATTTCCATTTTTCCCTAGACGCTG-3'

rev: 5'-TACCTCAGCTTCTTCTTGCTCTTT-3'

F1449V

for: 5'-TTATAGGTAGACAAGCAGCCCAAA-3'

rev: 5'-CCTAAATCATAAGTTAGCCAGAACC-3'

ArrayCGH analysis was performed with genomic DNA of iPSC clones and corresponding subject material using CytoSure™ ISCA v2 4x180k microarrays and analysed using Cytosure™ software (Oxford Gene Technologies, Begbroke, UK).

Immunocytochemistry

IPSC clones or sensory neurons were fixed in 4% paraformaldehyde for 20 min at RT, permeabilised in 0.3% Triton-X in PBS and blocked with 5% donkey serum/ PBS-T (Triton 0.1%). IPSC clonal lines were stained with primary antibodies anti-Oct4 (sc-8628, Santa Cruz, Dallas, Texas) and anti-Nanog (ab62734, Abcam, Cambridge, UK) overnight. Sensory like neurons were stained with anti-peripherin, anti-brn3a and anti-islet-1 (sc-7604 Santa Cruz, Dallas, Texas; ab5945; ab86501 Abcam, Cambridge, UK respectively) overnight. Cells were incubated with Alexa fluorophore secondary antibodies (Life Technologies, Carlsbad, California) in PBS-T for 1hr with intermediate washes. Nuclei were stained with Hoechst (Life Technologies, Carlsbad, California). Images were acquired on the Zeiss Observer ZI with Axiovision software (Zeiss, Jena, Germany) or Image Xpress platform (Molecular Devices, Sunnyvale, California).

Differentiation into sensory neurons

Differentiation into sensory neurons was performed as described previously[12,13]. Differentiated neurons were maintained for 8 weeks in neural growth factor medium comprising DMEM/F12 1:1 supplemented with 10% fetal bovine serum (Life Technologies, Carlsbad California) and 10 ng/ml nerve growth factor (NGF), brain-derived neurotrophic factor (BDNF), glial cell derived neurotrophic factor (GDNF), neurotrophin-3 (NT-3)

(Peprotech, Rocky Ville, New Jersey) and ascorbic acid (Sigma, St. Louis, Missouri). Medium was changed twice weekly.

Electrophysiology

IPSC-SN (typically eight weeks post growth factor addition) were dissociated and re-plated as described in Chambers *et al.,* (2012)[12]. Patch-clamp experiments were performed in whole-cell configuration using a patch-clamp amplifier 200B for voltage clamp and Multiclamp 700A or 700B for current clamp controlled by PClamp 10 software (Molecular Device, Sunnyvale, California). Voltage-clamp experiments were performed at room temperatue, while current-clamp experiments were performed at 35 °C or 40 °C using a CL-100 in-line solution heating system (Warner Instruments, Hamden, Connecticut).

Temperature was calibrated at the outlet of the in-line heater before each experiment. Patch pipettes had resistances between 1.5 and 2 MΩ. Basic extracellular solution contained (mM) 135 NaCl, 4.7 KCl, 1 CaCl2, 1 MgCl2, 10 HEPES and 10 glucose; pH was adjusted to 7.4 with NaOH. The intracellular (pipette) solution for voltage clamp contained (mM) 100 CsF, 45 CsCl, 10 NaCl, 1 MgCl2, 10 HEPES, and 5 EGTA; pH was adjusted to 7.3 with CsOH. For current-clamp the intracellular (pipette) solution contained (mM) 130 KCl, 1 MgCl2, 5 MgATP, 10 HEPES, and 5 EGTA; pH was adjusted to 7.3 with KOH. The osmolarity of solutions was adjusted to 320 mOsm/L for extracellular solution and 300 mOsm/L for intracellular solutions. All chemicals were purchased from Sigma Aldrich (St. Louis, Missouri). Currents were sampled at 20 kHz and filtered at 5 kHz. In voltage-clamp recordings between 80% and 90% of the series resistance was compensated to reduce voltage errors. The voltage protocol used to assess the effect of the compounds on voltage-gated sodium channels consisted of a step to -70 mV for 5 seconds from a holding potential of -110 mV, followed by a recovery step to -110 mV for 100 millisecond, followed by a test pulse to 0 mV lasting 20 milliseconds. Intersweep intervals were 15 seconds. Current threshold (or

rheobase) was measured in current-clamp mode by injecting 30 millisecond duration current steps of regularly increasing amplitude until a single action potential was evoked. The increasing current steps were in cycled sweeps to track the changes of current threshold (rheobase) while temperature was varied or compounds were applied to the cells. Intersweep intervals were 2 seconds. Two to three subclones were generated for each of the four IEM donors and four healthy donors. Excitability characterization data were pooled from all subclones of four IEM donors (individual subclones data can be seen in Supplementary Fig. 3D), while one subclone of each healthy donors was investigated.

Excitability was measured at resting membrane potential for each cell. The effect of compounds and temperature on rheobase was measured at a fixed membrane potential of -70 mV to avoid membrane potential changes induced error. Current-clamp data was analyzed using Spike2 software (Cambridge Electronic Device, UK), Prism 6.0 (Graphpad Software, La Jolla, California) and Origin 9.1 software (Originlab, Northampton, Massachusetts). Wherever possible the raw or derived data are presented. Exploratory analyses were performed to assess the difference between the average of the four IEM donors and the average of the four non-IEM donors. This contrast between the groups was fitted using a one way ANOVA for all responses except spontaneous firing, which was analysed using a linear logistic model; and rheobase, which was analysed using a non parametric ANOVA (Kruskal-Wallis test). All statistical analyses were carried out using SAS 9.4 (SAS Institute Inc. Cary, North Carolina).

REFERENCES

1. J. P. H. Drenth, S. G. Waxman, Mutations in sodium channel gene SCN9A cause a spectrum of human genetic pain disorders. *J. Clin. Invest*. **177**, 3603-3609 (2007).
2. S. D. Dib-Hajj, Y. Yang, J. A. Black, S. G. Waxman. The $Na_V1.7$ sodium channel: from molecule to man. *Nat. Rev. Neurosci*. **14,** 49-62 (2013).

3. D. L. Bennett, C. G. Woods. Painful and painless channelopathies. *Lancet Neurol.* **13**. 587-599 (2014).
4. A. McDonnell, B. Schulman, Z. Ali, S. D. Dib-Hajj, F. Brock, S. Cobain, T. Mainka, J. Vollert, S. Tarabar, S. G. Waxman. Inherited Erythromelalgia due to mutations in SCN9A: Natural History, Clinical Phenotype and Somatosensory Profile (*Brain*, in press) (2016).
5. T. R. Cummins, S. D. Dib-Hajj, S. G. Waxman. Electrophysiological properties of mutant Nav1.7 sodium channels in a painful inherited neuropathy. *J. Neurosci.* **24**, 8232-8236 (2004).
6. M. T. Wu, P. Y. Huang, C. T. Yen, C. C. Chen, M. J. Lee. A novel *SCN9A* mutation responsible for primary erythromelalgia and is resistant to the treatment of sodium channel blockers. *PLoS One.* **8**, e55212 (2013).
7. M. Estacion, Y. Yang, S. D. Dib-Hajj, L. Tyrrell, Z. Lin, Y. Yang, S. G. Waxman. A new Nav1.7 mutation in an erythromelalgia patient. *Biochem. Biophys. Res. Commun.* **432**, 99-104 (2013).
8. M. Eberhart, J. Nakajima, A. B. Klinger, C. Neacsu, K. Hühne, A.O. O'Reilly, A. M. Kist, A. K. Lampe, K. Fischer, J. Gibson, C. Nau, A. Winterpacht, A. Lampert. Inherited pain: sodium channel Nav1.7 A1632T mutation causes erythromelalgia due to a shift of fast inactivation. *J Biol Chem.* **289**, 1971-1980 (2014).
9. T. Stadler, A. O. O'Reilly, A. Lampert. Erythromelalgia Mutation Q875E Stabilizes the Activated State of Sodium Channel Nav1.7. J. *Biol. Chem.* In press (2015).
10. J. W. Theile, B. W. Jarecki, B. W, A. D. Piekarz, T. R. Cummins. Nav1.7 mutations associated with paroxysmal extreme pain disorder, but not erythromelalgia, enhance Nav beta4 peptide-mediated resurgent sodium currents. *J. Physiol.* **589**, 597-608 (2011).

11. S. D. Dib-Hajj, J. S. Choi, L. J. Macala, L. Tyrrell, J. A. Black, T. R. Cummins, S. G. Waxman. Transfection of rat or mouse neurons by biolistics or electroporation. *Nat. Protoc.* **4**, 1118-1126 (2009).

12. S. M. Chambers, Y. Qi, Y. Mica, L. Gabsang, X. J. Zhang, L. Niu, J. Bilsland, L. Cao, E. Stevens, P. Whiting, S. H. Shi, L.Studer. Combined small-molecule inhibition accelerates developmental timing and converts human pluripotent stem cells into nociceptors. *Nat. Biotechnol.* **30**, 715-720 (2012).

13. G. T. Young, A.Gutteridge, H. D. E. Fox, A. L. Wilbrey, L. Cao, L. T. Cho, A. R. Brown, C. L. Benn, L. R. Kammonen, J. H. Friedman, M. Bictash, P. Whiting, J. G. Bilsland, E. B. Stevens. Characterizing human stem cell-derived sensory neurons at the single-cell level reveals their ion channel expression and utility in pain research. *Mol. Ther.* **22**, 1530-1543 (2014).

14. M. Grskovic, A. Javaherian, B. Strulovici, G. Q. Daley, Induced pluripotent stem cells-opportunities for disease modelling and drug discovery. *Nat. Rev. Drug Discov*. **10**, 915-929 (2011).

15. J. McNeish, J. P. Gardner, B. J. Wainger, C. J. Woolf, K. Eggan, From Dish to Bedside: Lessons Learned While Translating Findings from a Stem Cell Model of Disease to a Clinical Trial. *Cell Stem Cell*. **17**, 8–10 (2015).

16. T. Z. Fischer, E. S. Gilmore, M. Estacion, E. Eastman, S. Taylor, M. Melanson, S. D. Dib-Hajj, S. G. Waxman, A novel Nav1.7 mutation producing carbamazepine responsive erythromelalgia. *Ann Neurol.* **65**, 733-741 (2009).

17. Y. P. Goldberg, N. Price, R. Namdari, C. J. Cohen, M. H. Lamers, C. Winters, J. Price, C. E. Young, H.Verschoof, R. Sherrington, S. N. Pimstone, M. R. Hayden, Treatmentof Na(v)1.7-mediated pain in inherited erythromelalgia using a novel sodium channel blocker. *Pain.* **153**, 80-85 (2012).

18. Y. P. Goldberg, C. J. Cohen, R. Namdari, N. Price, J. A. Cadieux, C. Young, R. Sherrington, S. N. Pimstone, Letter to the Editor. *Pain* **155**, 837-8(2014).

19. D. V. Vasylyev, C. Han, P. Zhao, S. Dib-Hajj, S. G. Waxman, Dynamic-clamp analysis of wild-type human Nav1.7 and erythromelalgia mutant channel L858H. *J. Neurophysiol.* **111**, 1429-1443 (2014).

20. S. D. DibHajj, A. M.Rush, T. R. Cummins,F. M. Hisama, S. Novella, L.Tyrrell, L.Marshall,S. G.Waxman, Gain-of-function mutation in Nav1.7 in familial erythromelalgia induces bursting of sensory neurons. *Brain.* **128**, 1847-1854 (2005).

21. C. Han, S. D. Dib-Hajj, Z. Lin, Y. Li, E. M. Eastman, L. Tyrrell. X. Cao, Y. Yang, S. G. Waxman. Early and late-onset inherited erythromelalgia: genotype-phenotype correlation. *Brain.* **132**, 1711-22 (2009).

22. Y. Yang, S. D. Dib-Hajj, J. Zhang, Y. Zhang, L. Tyrrell, M. Estacion ,S. G. Waxman, Structural modelling and mutant cycle analysis predict pharmacoresponsiveness of a Na (V)1.7 mutant channel. *Nat. Commun.*. **3**, 1186 (2012).

23. K. Ørstavik, C. Weidner, R. Schmidit, M. Schmelz, H. Hilloges, E. Jørum, H. Handwerker, E. Torebjörk, Pathological C-fibres in patients with a chronic painful condition. *Brain.* ***126****,567*-78 (2003).

24. O. Uyanik, C. Quiles, H. Bostock, S. D. Dib-Hajj, T. Fischer, L. Tyrrell, S. G. Waxman, J. Serra, Spontaneous impulse generation in C-nociceptors of familial erythromelalgia (FE) patients. *Eur. J. Pain.* **11**, S 130-293 (2007).

25. B. Namer, K. Ørstavik, R. Schmidt, I. P. Kleggetveit, C. Weidner, C. Mørk, M. S. Kvernebo, k. Knut ,H. Salter, T. H. Carr, M. Segerdahl, H. Quiding, Hans ,S. G. Waxman, H. O. Handwerker, H. E. Torebjörk, E. Jørum, M. Schmelz. Specific changes in conduction velocity recovery cycles of single nociceptors in an erythromelalgia patient with the I848T gain-of-function mutation of Nav1.7. *Pain.* **290**, 6316-6325, (2015).

26. J. J. Michiels, R. H. Te, Morsche, J. B. Jansen, J. P. Drenth. Autosomal dominant erythermalgia associated with a novel mutation in the voltage-gated sodium channel alpha subunit Nav1.7. *Arch. Neurol.* **62**, 1587-1590 (2005).

27. ClinicalTrials.gov [Internet]. Identifier:NCT02215252 A Clinical Trial To Evaluate PF-05089771 On Its Own And As An Add-On Therapy To Pregabalin (Lyrica) For The Treatment Of Pain Due To Diabetic Peripheral Neuropathy (DPN). Available from: https://clinicaltrials.gov/ct2/show/NCT02215252

Acknowledgements

We thank those subjects who participated in this study and their families for their support. We thank Dr Franco Di Cesare for medical input into this study and Stella Carolan and Joyce van Winkle for care of subjects and study management. We thank Zhixin Lin, David Printzenhoff, Mark Chapman and Neil Castle for PatchXpress characterization of PF-05089771 and PF-5153462.

We thank Roslin Cells Ltd. for generation of some of the iPSC lines used in this study.

The research leading to these results has received support from the Innovative Medicines Initiative Joint Undertaking under grant agreement n° 115439, resources of which are composed of financial contribution from the European Union's Seventh Framework Programme (FP7/2007-2013) and EFPIA companies' in kind contribution. MM was supported by an Industrial CASE PhD studentship from the Biotechnology and Biological Sciences Research Council (BBSRC) in partnership with Pfizer.

This publication reflects only the authors' views and neither the IMI JU nor EFPIA nor the European Commission are liable for any use that may be made of the information contained therein.

This study was funded by Pfizer Inc.

The Clinicaltrials.gov registration number for this study is NCT01769274[27].

Patient derived lines are deposited in the European Bank for Induced pluripotent stem cells (EBiSC: https://www.ebisc.org/) to whom initial enquiries for access should be addressed. The EBiSC project has received support from the Innovative Medicines Initiative Joint Undertaking under grant agreement n° 115582, resources of which are composed of financial contribution from the European Union's Seventh Framework Programme (FP7/2007-2013) and EFPIA companies' in kind contribution.

Table 1. IEM Subject Clinical Phenotype.

Subject ID	SCN9A mutation	Gender	Age at onset of IEM (yr)	Pain attack trigger	Consent* to donate blood for iPSC
EM1	S241T	F	17 yr	Heat, Exercise	Yes
EM2	I848T	M	4 yr	Heat, Exercise	Yes
EM3	V400M	M	>10 yr	Heat, Exercise, Standing	Yes
EM4	V400M	M	4 yr	Heat, Exercise,	No
EM5	F1449V	F	< 2 yr	Heat, Exercise, Standing	Yes

*Consent to donate blood for iPSC generation was optional for subjects in the clinical study

Fig.1. IPSC from IEM subjects and non-IEM donors differentiate to sensory neurons with comparable Nav1.7 activity.

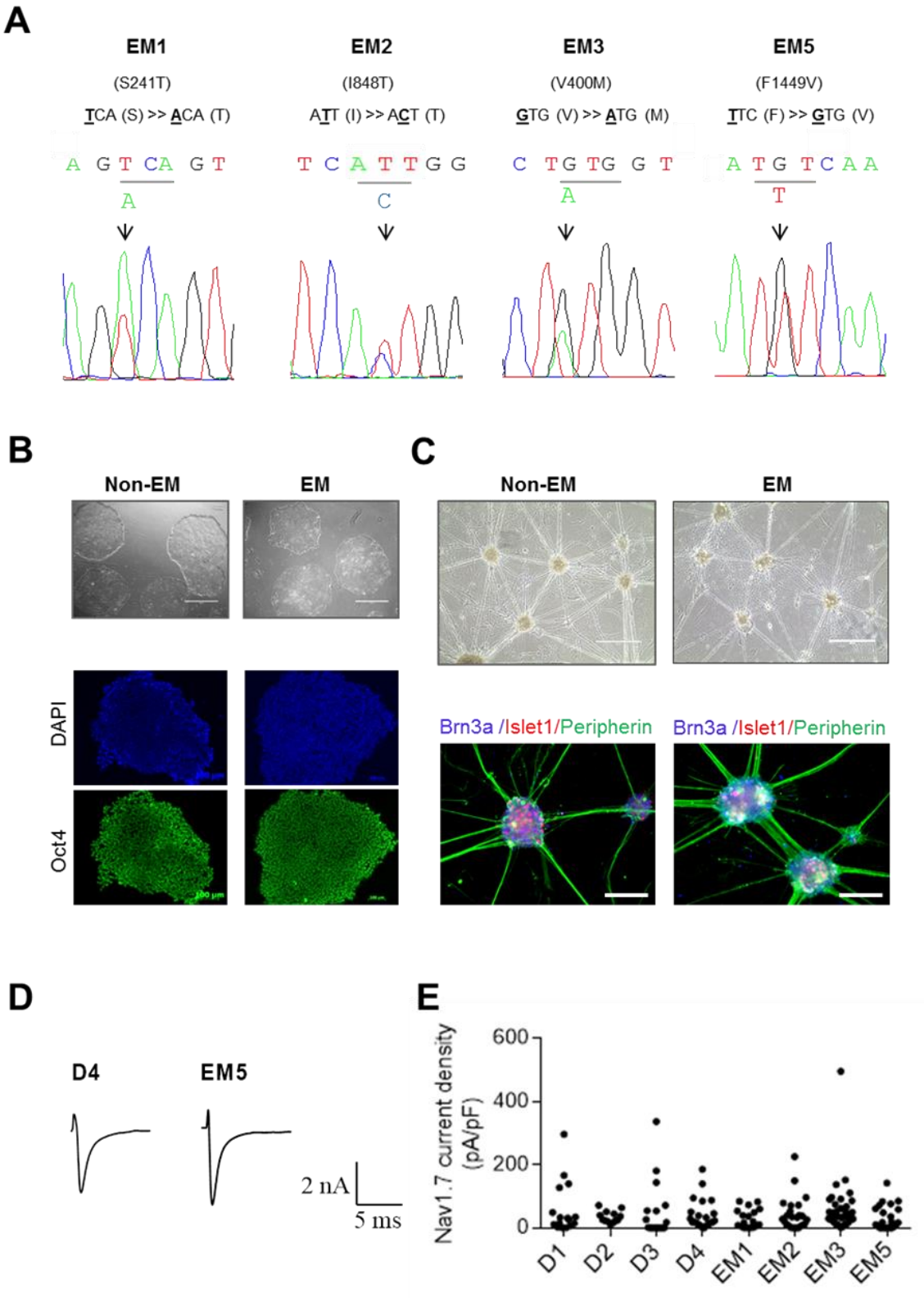

(**A**) Confirmation of mutations in respective IEM subject-derived iPSC by Sanger sequencing. The arrow highlights the heterozygous point mutation in the pherogram. (**B**) Representative examples of IEM subject and non-IEM donor derived iPSC showing typical pluripotent-like morphology and expression of pluripotent marker Oct4. Scale bar equals 1000 µm and 100 µm respectively. (**C**) Representative examples of IEM subject and non-IEM donor derived iPSC differentiated into sensory-like neurons. Scale equals 1000 µm. Immunostaining confirms expression of sensory neuron marker Brn3a, Islet1 and Peripherin. Scale bar equals 200 µm. (**D**) Example traces measured in the non EM donor (D4) and EM subject (EM5; F1449V) derived iPSC-SN showing the selective Nav1.7 blocker sensitive current components. Cells were held at -110 mV and stepped to 0 mV to evoke voltage gated currents which were partially blocked by 100 nM PF-05153462. (**E**) Summary of Nav1.7 current density in the non-IEM donors and IEM subject derived IPS sensory neurons. No significant difference was observed among all the clones (*N*= 13 to 40).

Fig. 2. IEM Subject-derived IPSC sensory neurons showed greater excitability compared to non-IEM donor clones.

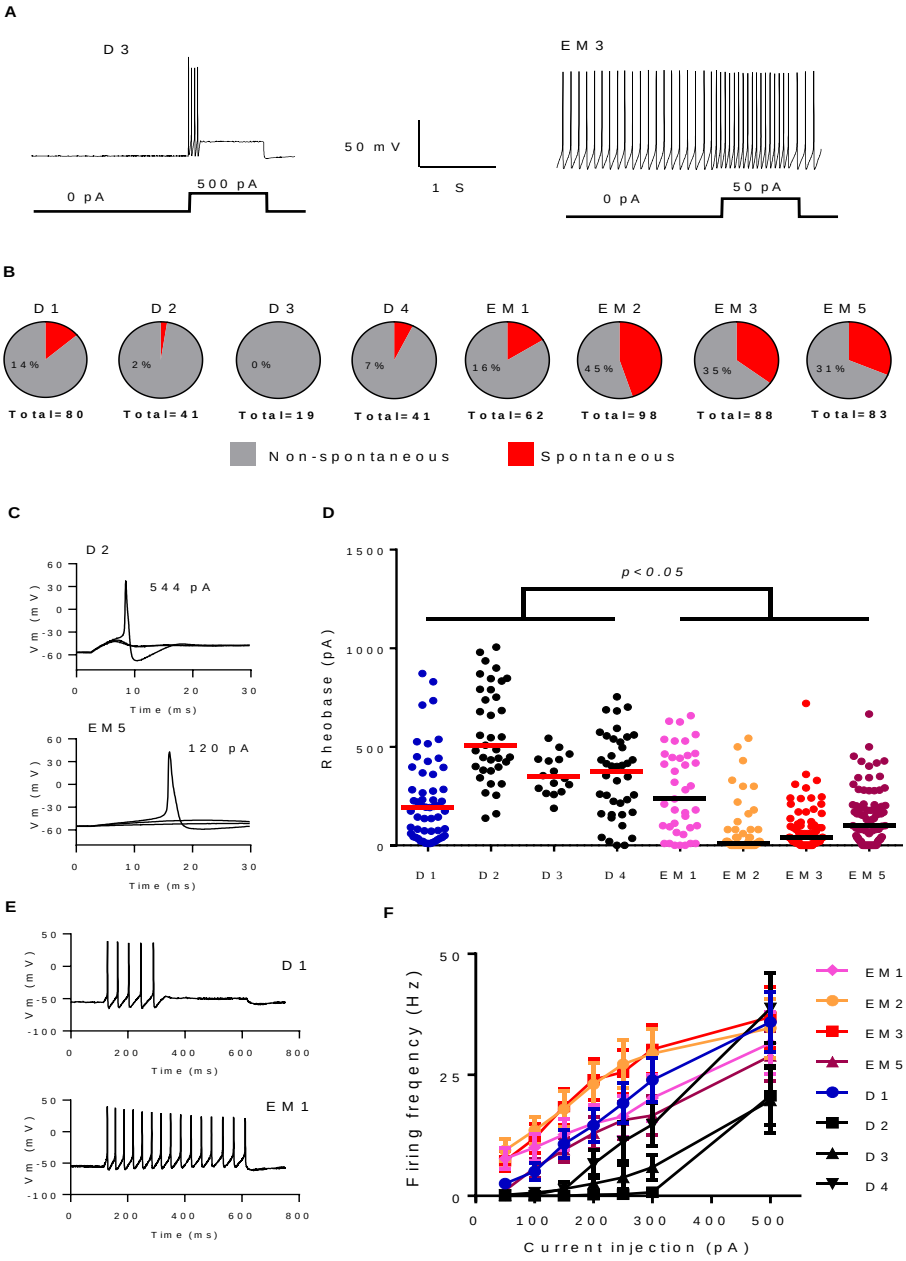

(**A**) Representative traces of spontaneous firing in EM3 (V400M) but not in D3 cells. (**B**) Quantification of number of spontaneous firing cells versus non-spontaneous cells in IPSC-SN (*N*=19 to 98*; P*<0.05 comparing average non-IEM donor clones and IEM subject clones using logistic regression). (**C**) Representative current clamp traces, showing subthreshold

responses and subsequent action potentials evoked until reaching current threshold (rheobase) of 544 pA for D3 and 120 pA for EM5 (F1449V) cells. (**D**) Quantification of action potential rheobase (N=16 to 86; P <0.05 comparing average healthy donors clones and IEM subjects' clones using non parametric ANOVA). (**E**) Representative traces showing train of action potentials evoked in D1 and EM1 (S241T) cells by 100 pA current injection induced depolarization. (**F**) Quantification of action potential frequency induced by current injection(N=10 to 46).

Fig. 3. Nav1.7 blockers reduced spontaneous firing and increased action potential rheobase in iPSC sensory neurons.

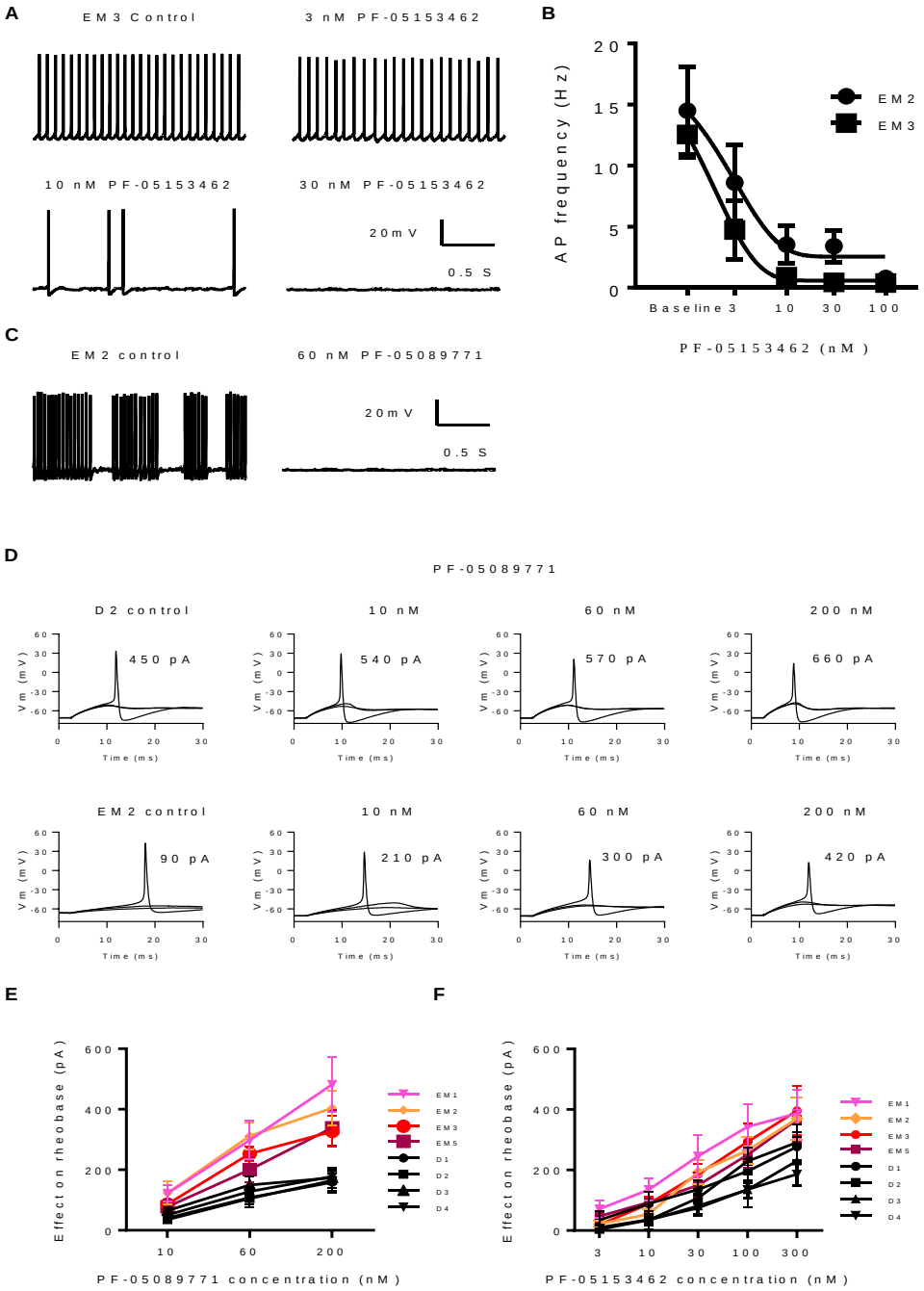

(**A**) Representative traces of spontaneous action potentials in EM3 (V400M)cells blocked by increasing concentration of PF-05153462. (**B**) Concentration-dependent effect of PF-05153462 on spontaneous firing with EC_{50} of 2 nM for both EM2 (I848T) and EM 3

(V400M) cells. (**C**) Representative traces of spontaneous firing blocked by 60 nM PF-05089771 on EM2 cells. (**D**) Representative current-clamp traces showing rheobase in D2 and EM2 (I848T) cells were elevated by application of PF-05089771 in a concentration-dependent manner. (**E**) Quantification of the effect of PF-05089771 on rheobase (N=6 to 10; P <0.05 comparing average non-IEM donor clones and IEM subject clones using ANOVA at each concentration). (**F**) Quantification of the effect of PF-0153462 on rheobase (N=6 to 10; P<0.05 comparing average non-IEM donor clones and IEM subject clones using ANOVA at each concentration greater than 10 nM).

Fig. 4. Nav1.7 blocker reversed the elevated heat sensitivity in IEM-derived IPSC sensory neurons.

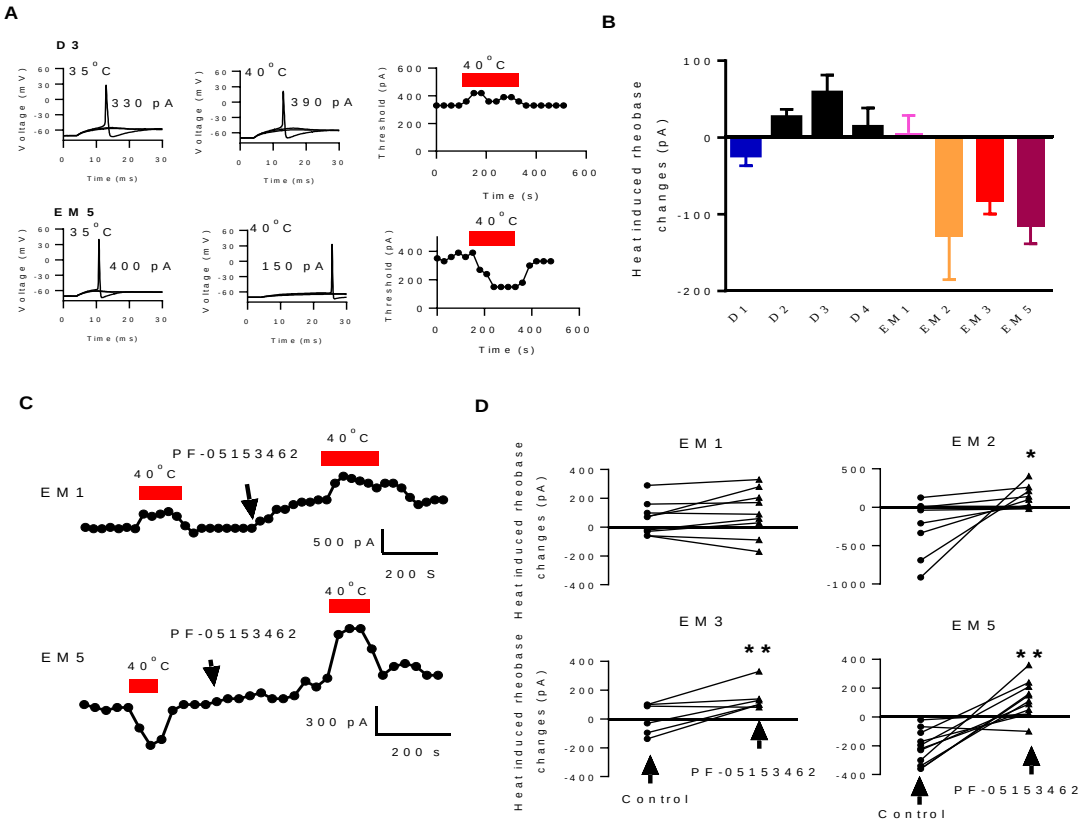

(A) Representative traces of evoked action potentials showing a small increase of rheobase when D3 neurons were incubated with extracellular recording solution at an elevated temperature of 40 °C from control temperature at 35 °C. In contrast, the rheobase on EM5 (F1449V) cells was decreased by the same heating procedure. Right panels show example time course of rheobase changes of D3 and EM5 (F1449V) cells upon heating. (**B**) Quantification of the effect heating on IPSC derived neurons. The heating effect was calculated as the change in the rheobase at 40 °C versus 35 °C (*N*=13 to 34; *P* <0.01; comparing average non-IEM donor clones and IEM subject clones using ANOVA). (**C**) Representative traces of rheobase showing the effect of heating on rheobase before and after the application of PF-05153462. The heat

sensitivity of rheobase was reversed by PF-05153462 on EM5 cells but no effect was seen on EM1 cells. (**D**) Quantification of the effect of PF-05153452 on heat sensitivity (*N*=6 to 10; *P >0.05* for EM1 (S241T), *P* <0.05 for EM2 (I848T), *P <0.01* for EM3 (V400M) and EM5 (F1449V) using paired t-test). Only cells demonstrating a positive response to PF-05153452 (where the rheobase showed sensitivity greater than 50 pA at 35^{o}C) were included and the number of cells excluded were 3 out 12 cells for EM1, 2 out of 10 cells for EM2, 1 out of 8 cells for EM3 and 1 out of 11 cells for EM5.

Fig. 5. Nav1.7 is the major contributor for the elevated heat sensitivity in IEM iPSC-SN

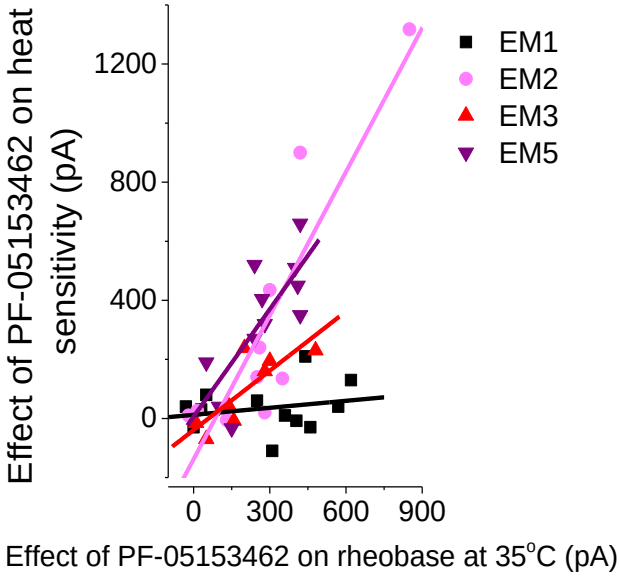

Correlation of the heat sensitivity changes to rheobase changes at 35°C induced by PF-05153462 (Pearson's correlation coefficients, r=0.22, 0.88, 0.82 and 0.77 for EM1, EM2, EM3 and EM5 respectively). The regression coefficients were significantly different to zero for EM2, EM3 and EM5, linear regression). In contrast to Figure 4**D**, both PF-05153462 positive cells (rheobase changes at 35°C greater than 50 pA, indicating clear Nav1.7 expression) and negative cells (rheobase changes at 35°C less than 50 pA, indicating low or no Nav1.7 expression) were all included.

Fig. 6. Clinical Study Design Overview and Maximum Pain Scores postdose.

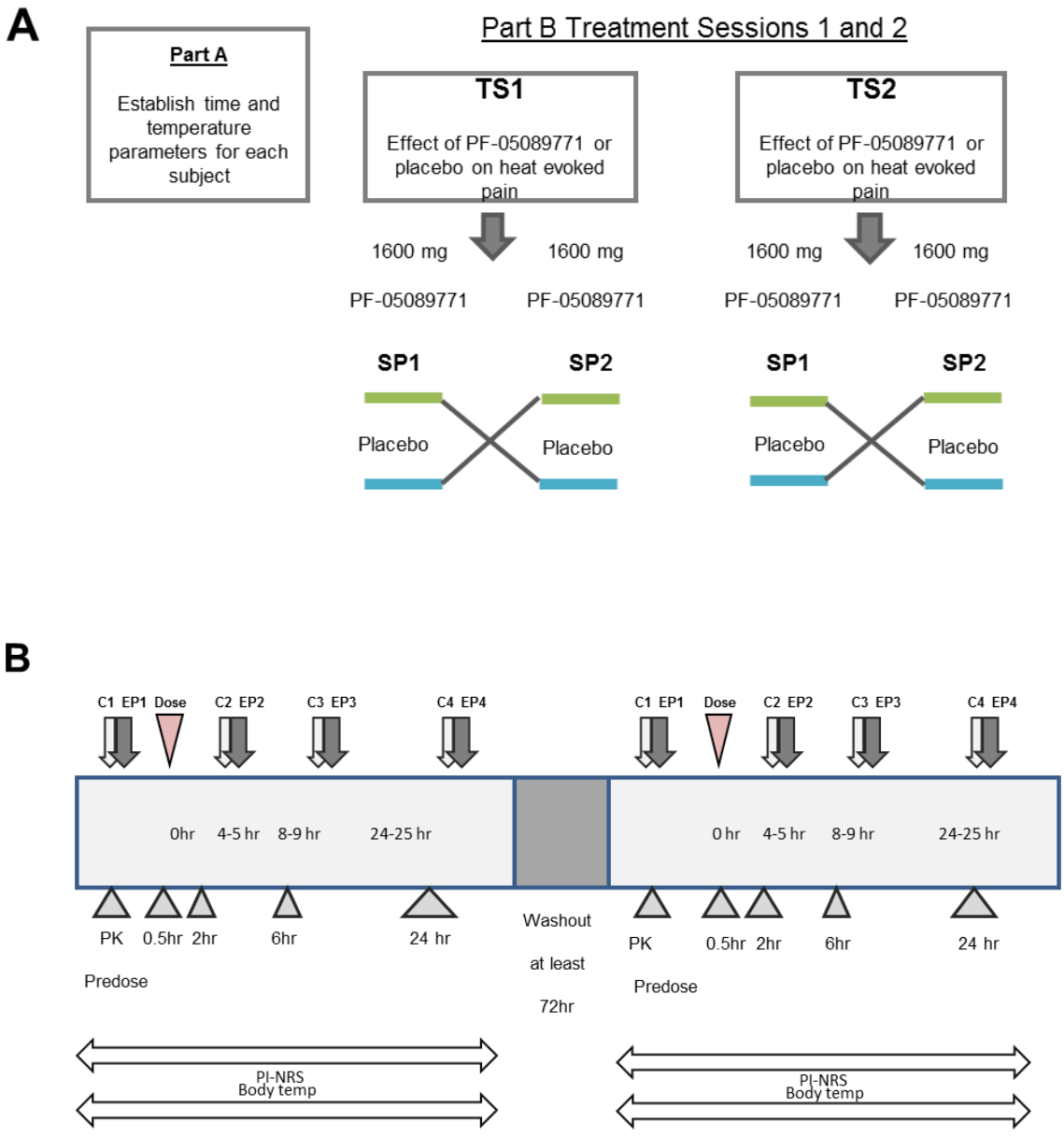

C

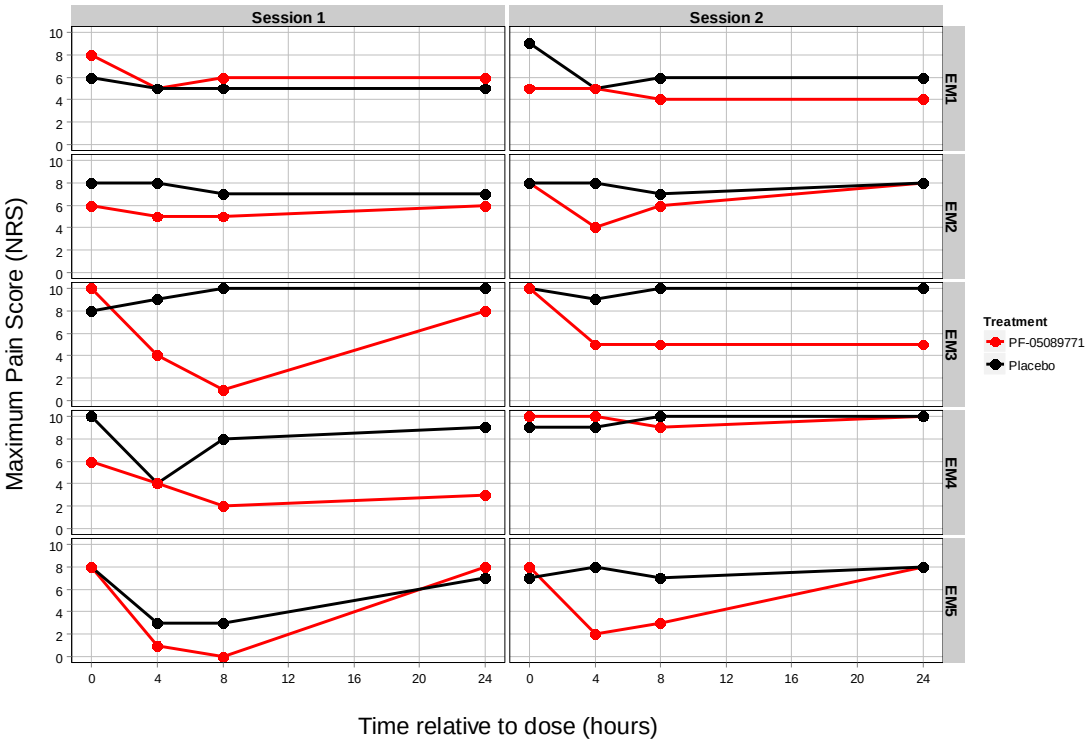
Session 1
Session 2
EM1
EM2
EM3
EM4
EM5
Maximum Pain Score (NRS)
Time relative to dose (hours)
Treatment
PF-05089771
Placebo

D

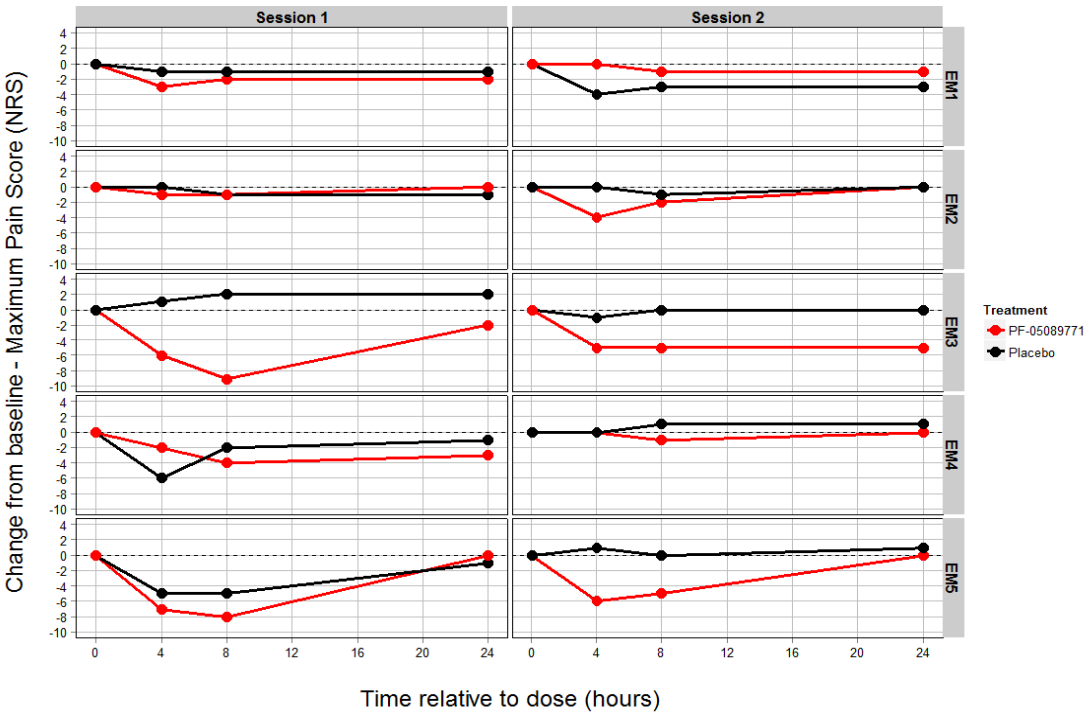
Session 1
Session 2
EM1
EM2
EM3
EM4
EM5
Change from baseline - Maximum Pain Score (NRS)
Time relative to dose (hours)
Treatment
PF-05089771
Placebo

E

Difference in Maximum Pain Scores Postdose (Includes subjects who used cooling as rescue therapy)				Difference in Maximum Pain scores Postdose (Excludes subjects who used cooling as rescue therapy)			
Time postdose	P value	Treatment Difference (PF-05089771 – Placebo)	90% Confidence interval	Time postdose	P value	Treatment Difference (PF-05089771 – Placebo)	90% Confidence interval
0-4 hr	0.49	-0.33	-1.17, 0.51	0-4 hr	0.74	0.25	-1.17, 1.67
4-5 hr	0.06	-2.56	-4.74, -0.39	4-5 hr	0.04	-3.13	-5.43, -0.82
8-9 hr	0.03	-3.63	-6.24, -1.01	8-9 hr	0.08	-3.63	-6.91, -0.34
24-25 hr	0.47	-0.77	-2.84, 1.29	24-25 hr	0.47	-0.77	-2.84, 1.29

(A) This 2-part study consisted of Parts A and B. Part A established individual subject evoked heat pain attack parameters using a controlled heat stimulus on at least 2 occasions. Part B consisted of two treatment sessions (TS1 and TS2), minimum 72 hr washout period between last treatment in TS1 and first treatment in TS2, maximum of up to 6 mth between TS1 and TS2.

(B) Each Treatment Session (TS) consisted of 2 study periods (SP). Subjects received either a single oral dose of PF-05089771 or placebo in a crossover manner in each SP. Pain scores were recorded every 15 min up to 10 hr postdose. Core body temperature was measured regularly throughout. Pharmacokinetic samples were collected predose and at 0.5 hr, 2 hr, 6 hr and 24hr postdose.

(C) Maximum pain scores recorded by subjects using the PI-NRS following dosing with either PF-05089771 or placebo in TS1 and TS2. Individual subject results for maximum pain scores includes subjects who used non-pharmacological rescue therapy. Subject EM1 (S241T) did not show any notable difference in pain scores for PF-05089771 versus placebo between TS1 and TS2. Subject EM2 (I848T) had reduction in pain scores in TS2 on PF-05089771 versus placebo at the 4-5 hr timepoint postdose. Subject EM4 (V400M) had

reduction in pain score at the 4-5 hr and 8-10 hr timepoint postdose in TS1, but no difference in pain scores between drug and placebo in TS2. Subjects EM3 (V400M) and EM5 (F1449V) had reduction in pain scores after a single dose of PF-05089771 at the 4-5 hr timepoint and the 8-10 hr timepoint postdose in both TS1 and TS2.

(D) Change from baseline in Maximum Pain Scores (PI-NRS) for PF-05089771 versus placebo in individual subjects.

(E) Differences in maximum pain scores postdose, including and excluding subjects who used cooling as "rescue" therapy**.**